American Mineralogist, Volume 62, pages 966–978, 1977

Relation of nucleation and crystal-growth rate to the development of granitic textures

SAMUEL E. SWANSON[1]

Tuttle-Jahns Laboratory for Experimental Petrology
and Geology Department, Stanford University
Stanford, California 94305

Abstract

Analysis of crystal growth as a function of temperature for synthetic granite and granodiorite compositions in the system $KAlSi_3O_8$–$NaAlSi_3O_8$–$CaAl_2Si_2O_8$–SiO_2 under H_2O-saturated and undersaturated conditions yields quantitative data on the growth kinetics of quartz, alkali-feldspar, and plagioclase in these systems at 8 kbar and 400–900°C. Measured growth rates vary from 3×10^{-6} cm/sec (about 3 mm/day) to 1×10^{-10} cm/sec (about 1 mm/yr), while nucleation density (nucleation sites/unit volume) varies from 0 to over 1×10^{8}sites/cm^3. Crystal-growth rates commonly increase with increased undercooling. Maximum growth rates are lower in systems which contain a H_2O-rich vapor phase than in systems that are undersaturated with respect to H_2O.

Number of nuclei (nucleation density), growth rate, and morphology for each of the minerals determines the texture of an igneous rock. Results of this study show that long periods of time are not *necessary* to produce the textures commonly associated with igneous rocks. A relatively small number of large crystals may be produced by crystallization at a low undercooling in a few days. Volcanic (fine-grained) textures may be produced by crystallization at large undercoolings, which produces a large number of small nuclei (high nucleation density, low growth rate). Coincidence of low nucleation density and high growth rate for alkali feldspar may explain the large alkali-feldspar crystals (phenocrysts or interstitial masses) sometimes found in granodiorites.

Introduction

Development of textures in igneous rocks has received relatively little study compared to various aspects of phase equilibria. Crystallization of magma involves the kinetics of nucleation, and crystal growth and useful concepts concerning these variables were developed many years ago (Tammann, 1925) to describe the crystallization of organic liquids. Empirical use of crystallization kinetics (Dowty *et al.*, 1974: Carmichael *et al.*, 1974) places restrictions on some models of igneous textural evolution. The purpose of this paper is to quantify nucleation and crystal-growth kinetics for some specific granitic systems. A better understanding of crystallization kinetics in geologically interesting systems should provide some models for the evolution of various igneous textures.

Theory

Theoretical analysis of nucleation and crystal growth is the subject of a large amount of literature. Tammann (1925) discussed the theory of nucleation and crystal growth, and outlined the various parameters involved in terms of a probabilistic model involving a functional relation to pressure, temperature, and time. Many later studies deal with the nucleation and growth of crystals on an atomistic level. Although such studies are very significant, data on nucleation and crystal-growth kinetics are required for the system under study prior to development of atomistic models. Quantitative data on nucleation and crystal growth are available for only a few systems of geological importance, and the purpose of this section is to present a brief introduction to theories of nucleation and crystal growth as a prelude to the results of crystal-growth experiments.

Nucleation involves the addition of atoms or molecules to a nucleus having the structure of the solid. If the nucleus is larger than a certain critical size, it will

---

[1] Present address: Geology Department, Appalachian State University, Boone, North Carolina 28608.

grow spontaneously, but if it is smaller than the critical size, the nucleus will be unstable. Critical size is dependent upon the amount of undercooling [$\Delta T = T$ (liquidus)$-T$ (growth)] and varies from an infinite size at liquidus temperatures to smaller sizes at greater degrees of undercooling. Another factor in the nucleation of crystals from a melt is the mobility of atoms and molecules in the melt as measured by the diffusion coefficient. In glass-forming systems, such as silicates, liquid diffusion coefficients drop markedly with decreasing temperature (Towers and Chipman, 1957). As the temperature drops below the liquidus, nucleation will increase from zero to a maximum at some undercooling. Diffusion rates are then very low and nucleation decreases with further decrease in temperature. This explains the pattern of nucleation in liquids where the liquid diffusivity decreases with temperature, and is consistent with the patterns observed in this study.

Crystal growth from a melt proceeds by attachment of chemical species from the liquid to the crystal nuclei. Rate of growth is thus a function of mobility of crystal-forming species within the melt. Mobility, as measured by the diffusion coefficient, drops with decreasing temperature, and growth rate, like nucleation, is expected to rise from zero at the liquidus to a maximum at some undercooling and then decrease. This is the expected pattern of growth rate of crystals from a viscous liquid (Tammann, 1925). For an excellent review of crystal growth in geological systems, the reader is referred to Kirkpatrick (1975).

Crystal morphology is a function of growth rate (Y) and mobility of the slowest crystal-forming component in the melt (D) (Kirkpatrick, 1975). Diffusion coefficients in a melt decrease with increased undercooling while, as previously explained, crystal-growth rate will increase to a maximum and then decrease. The net result is that D/Y decreases with increased undercooling (Kirkpatrick, 1975). At small undercoolings D/Y is relatively large, and crystals are expected to have smooth, planar surfaces (Cahn, 1967; Kirkpatrick, 1975). With increased undercooling D/Y decreases causing a breakdown of smooth, planar crystal faces. Initially the breakdown of planar crystal faces takes the form of widely-spaced protuberances on the crystal faces, and with increased undercooling the spacing between the protuberances decreases. The pattern of crystal morphology is expected to change from smooth, planar crystal faces at low undercoolings to spherulitic crystals at large undercoolings (Keith and Padden, 1963; Kirkpatrick, 1975).

Previous work

Research on nucleation and crystal growth in silicate systems has been done primarily by material scientists in connection with the ceramic and glass industries. Some of these studies, *e.g.* Meiling and Uhlmann (1967), have used seed crystals in growth-rate experiments and thus are not concerned with the nucleation of crystals.

A few crystal-growth studies at one atmosphere pressure with anhydrous bulk compositions have dealt with applications to naturally occurring crystals. Vogt (1923) recognized the rapid growth rate (on the order of 1 mm/min) of akermanite, diopside, fayalite, and rhodonite from a silicate liquid. Winkler (1947) measured the growth rate of nepheline in the system Na_2CO_3–Al_2O_3–SiO_2–LiF. More recently, Kirkpatrick (1974) studied the growth rate of pyroxene, anorthite, and melilite in the system $CaMgSi_2O_6$–$CaAl_2SiO_6$. Gibb (1974) found the nucleation of plagioclase varied as a function of temperature, time, and cooling rate. Kirkpatrick *et al.* (1975) measured the rate of growth of diopside and anorthite from melts of their own composition, and also found that diopside nucleates more readily than plagioclase. Extension of the crystal-growth studies to high-pressure systems seems natural, but has been tried by only a few researchers.

Most crystal-growth studies at elevated pressures have been concerned with textural relations rather than nucleation and crystal-growth kinetics. Jahns and Burnham (1958) grew crystals from a hydrous silicate liquid formed by melting a sample of natural pegmatite, as pictured in Wyllie (1963). Mustart (1969) grew crystals of albite in the system $NaAlSi_3O_8$–$Na_2Si_2O_5$–H_2O. Substitution of $KAlSi_3O_8$ or SiO_2 for $NaAlSi_3O_8$ allowed growth of potassium feldspar and quartz respectively (Mustart, 1969, 1972). Swanson *et al.* (1972) grew crystals of plagioclase, alkali-feldspar, and quartz in hydrous haplogranitic systems. Lofgren (1974a,b) has grown plagioclase crystals in the system $NaAlSi_3O_8$–$CaAl_2Si_2O_8$–H_2O. Donaldson (1974) studied the texture of olivine crystals grown from feldspathic peridotite and quartz-normative basalt systems. Lofgren *et al.* (1975) have investigated the development of porphyritic texture in terrestrial and lunar basaltic compositions. Naney (1975) has grown biotite and clinopyroxene from haplogranitic liquids. These studies show the feasibility of studying crystal growth in silicate systems of geologic importance.

Kinetics of nucleation and growth of alkali-feldspars from a hydrous silicate liquid in the system $KAlSi_3O_8$–$NaAlSi_3O_8$–H_2O have been intensively studied by Fenn (1972, 1973, 1976), following the method of Mustart (1969). Experiments were made with both H_2O-undersaturated and saturated silicate liquids. Growth rates were relatively high (up to 6.8×10^{-6}cm/sec). Nucleation lag times of up to 48 hours indicate that the measured growth rates are minimum values. Growth rates in the liquid plus aqueous vapor assemblages were lower than in the undersaturated bulk compositions.

The relation of crystal-growth rate and nucleation density to igneous textures was described by Swanson (1974) in relation to a haplogranodiorite composition. Growth rates ranged from 1.4×10^{-6} to 1×10^{-10} cm/sec for the plagioclase crystals, while the quartz and potassium feldspar crystals had maximum growth rates of about 2×10^{-7} cm/sec. Relative positions of the growth rate and nucleation curves were used to explain igneous textures.

Selection of bulk compositions

Preliminary experiments (Swanson *et al.,* 1972) had shown the feasibility of growing crystals from hydrous silicate liquids in the haplogranitic systems. In order to assess the role of anhydrous bulk composition on nucleation and crystal growth, synthetic granite and granodiorite compositions were selected for study as representing a variety of phase assemblages. These compositions were modeled in the system $NaAlSi_3O_8$–$KAlSi_3O_8$–$CaAl_2Si_2O_8$–SiO_2 after the granite and granodiorite in the hornblende-biotite series of Nockolds' (1954). The compositions are given in Table 1. Whitney (1975) has studied the effect of pressure, temperature, and water content on the phase relations of these bulk compositions, and Figure 1 shows the results of the 8000 bar experiments and the systems selected for study.

Table 1. Chemical compositions studied

Oxide	Synthetic granite	Synthetic granodiorite
SiO_2	73.98	70.34
Al_2O_3	15.07	18.00
CaO	1.50	3.97
Na_2O	3.75	4.37
K_2O	5.70	3.32
Modified normative equivalent		
Q	26.5	23.1
Or	34.0	19.8
Ab	32.0	37.3
An	7.5	19.8

Experimental method

Experiments were made in internally-heated pressure vessels modified considerably from the design of Yoder (1950). Temperatures were measured with Pt/Pt-10 Rh thermocouples periodically calibrated against the melting points of gold (1062.5°C) and sodium chloride (800.5°C). Pressure corrections were made in thermocouple calibration using the data of Clark (1959) and Akella and Kennedy (1971). Temperature measurements are probably precise to ±10°C, and the pressure measurements made with manganin coils are thought to be ±100 bars.

Dehydrated silicate gels (Luth and Ingamells, 1965) were used as the starting materials. Gels were dried in a vacuum oven prior to loading. Water distilled, deionized, and boiled just prior to use was added to platinum or $Ag_{60}Pd_{40}$ capsules (2.0 mm O.D.) sealed at one end. A calculated amount of dried gel was added and the capsule sealed by welding. Capsules were then placed in a vacuum oven to check for leaks and to distribute the fluid homogeneously throughout the charge. Two capsules of the same composition were loaded and run in each experiment to allow for the low probability of nucleation in some compositions ('experiment' refers to a group of capsules that were contained in the same pressure vessel at the same time, and 'charge' refers to the content of a single capsule).

Capsules were allowed to homogenize for not less than 96 hours above the liquidus at 1000°C (Fig. 1). Then the temperature was dropped to the isotherm selected for nucleation and growth. Time required for the drop to the growth temperature varied with the amount of undercooling but was on the order of a few minutes. During quench to the growth isotherm, pressure could not be maintained isobaric due to limitations of the pumping system, pressure drops as large as 2000 bars resulted. Following the drop in temperature to the growth isotherm, pressure was readjusted to 8000 bars. Capsules remained at the growth isotherm for 24 to 144 hours, and the experiment was then quenched to room temperature by turning off the furnace power. This resulted in a temperature drop of 300°C after 10 minutes; room temperature was reached within 20 minutes.

It may be argued that the pressure used in this study (8000 bars) limits the applicability of the re-

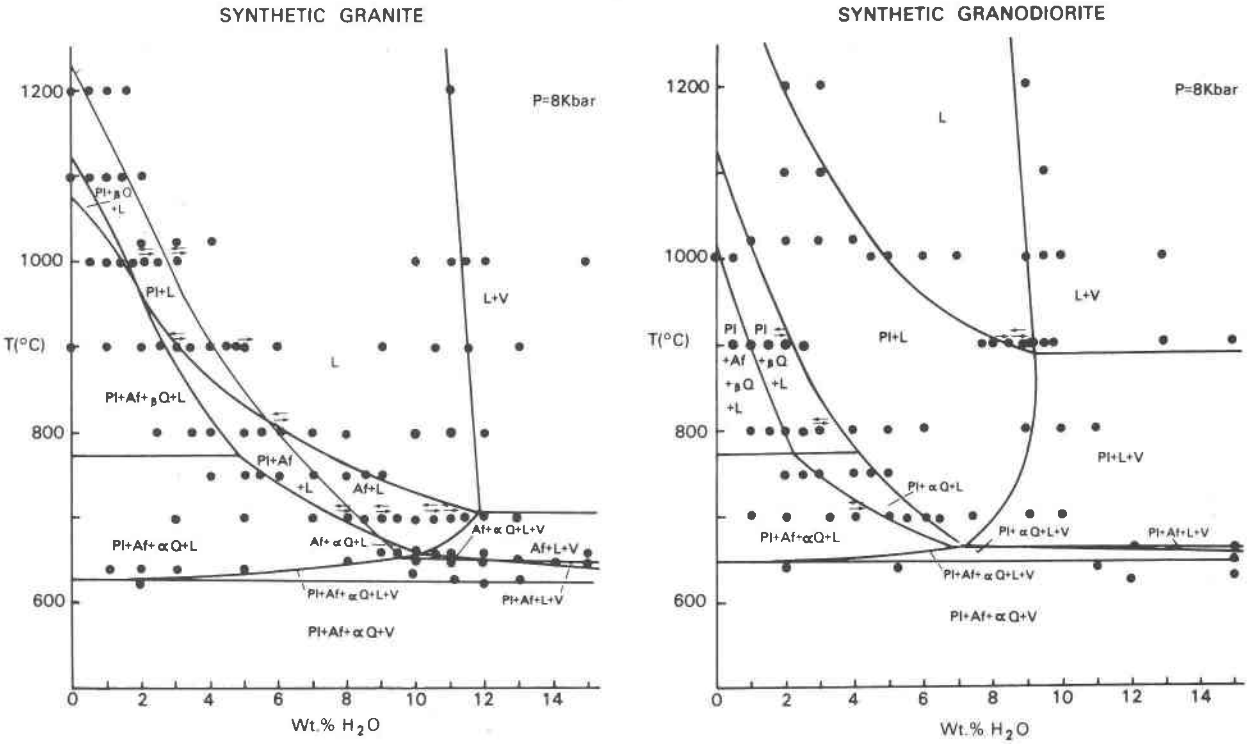

Fig. 1. Bulk compositions selected for crystal growth. (a) Temperature *vs.* wt % H_2O phase-assemblage diagram for synthetic granite (Whitney, 1975). (b) Temperature *vs.* wt % H_2O phase-assemblage diagram for synthetic granodiorite (Whitney, 1975).

sults. This pressure was selected: (1) to take advantage of the depression of liquidus temperatures at high pressure, and (2) because the phase relations for these compositions were well known at this isobar (Whitney, 1975). Reconnaissance experiments at 2000 bars suggest the *form* of the curves shown on Figures 2 and 3 is little changed by pressure, though the absolute values may be changed.

Results

Experiments were done at 50° intervals from 900° to 600°C and at 100° intervals from 600°C to 400°C, and are more successful with the granodiorite compositions than with the granite compositions. At higher water contents the granite compositions often fail to nucleate any crystals, and only the granite composition plus 3.5 weight percent water yield sufficient data for a meaningful analysis.

Nucleation

After the capsules were opened, the charges were examined with the microscope and the number of nucleation sites were counted or estimated. Charges and quartz grains were embedded in epoxy, and a thin section was prepared with the quartz used to gauge the thickness. Nucleation sites were then counted in a portion of the charge, and the use of the thickness of the thin section resulted in an estimate of the nucleation sites as a function of volume. In charges with only a few nucleation sites the total number of sites were counted, and this was divided by the average volume of the charges (about 0.032 cm^3) to obtain the nucleation density. Results of the nucleation density measurements are shown on Figure 2 as a function of temperature. Attempts to determine rates of nucleation were made by determining the nucleation density as a function of time for a given isotherm and bulk composition. However, lack of nucleation during the experiment made it very difficult to determine nucleation rates (Table 2). Thus the number of nucleation sites present at the end of the experiment was the only nucleation parameter that could be routinely determined for all charges with crystals. When nucleation-rate data could be obtained, they followed the general pattern shown by the nucleation density on Figure 2.

When the charges are examined, the probabilistic nature of the nucleation is readily apparent. Variation in growth time probably accounts for the considerable scatter in the nucleation density data; for ex-

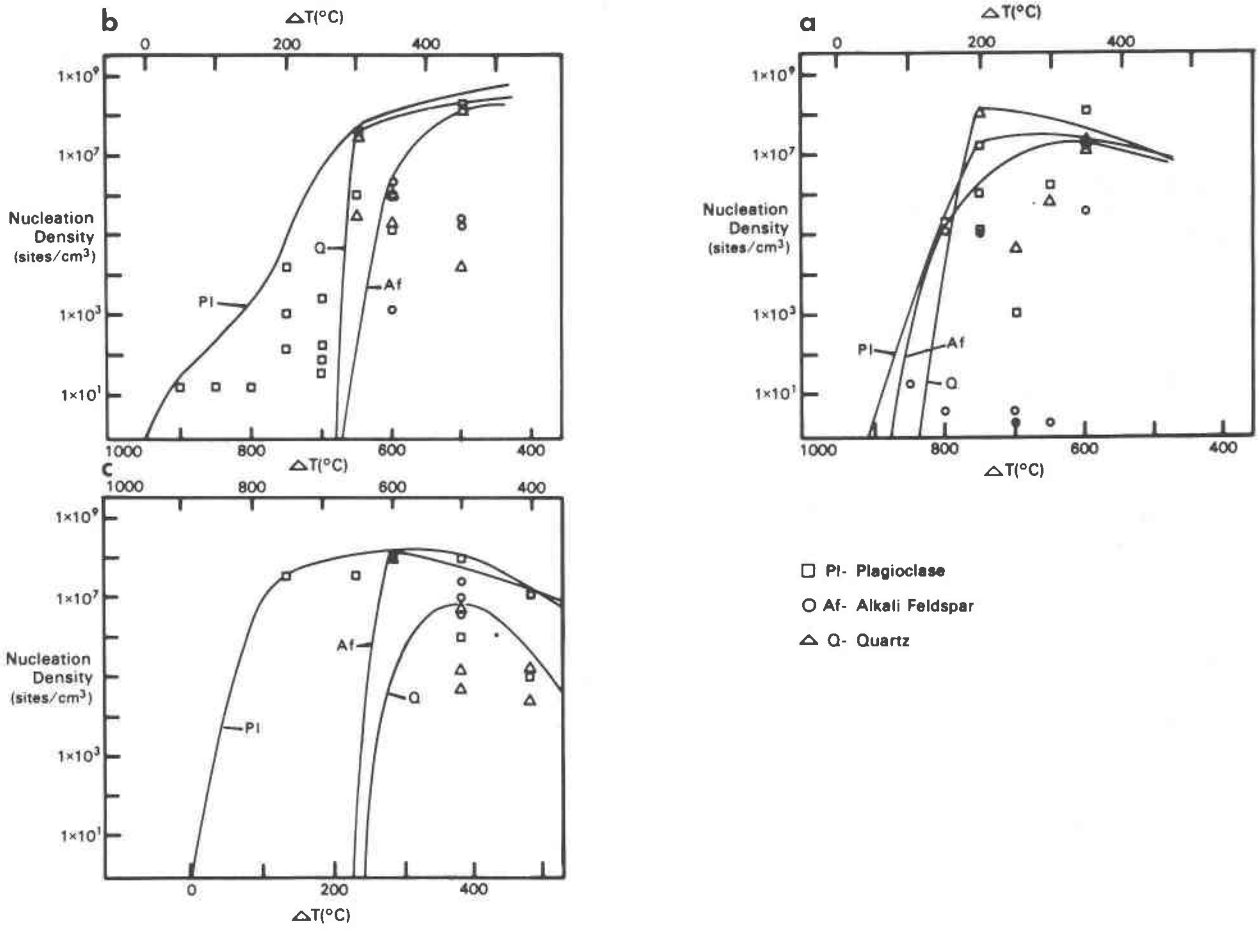

Fig. 2. Nucleation density as a function of undercooling (ΔT). (a) Synthetic granite plus 3.5 wt % H_2O. (b) Synthetic granodiorite plus 6.5 wt % H_2O. (c) Synthetic granodiorite plus 12 wt % H_2O. (c) Synthetic granodiorite plus 12 wt % H_2O.

ample in short-duration experiments one charge often shows nucleation whereas the other charge does not contain any crystals (Table 2). Curves for nucleation density shown on Figure 2 have been constructed from the maximum values only in an attempt to escape the scatter. These curves probably reflect the form of the nucleation density, but due to the considerable scatter of data the absolute maximum and location of the curves cannot be determined.

Time lag between quench to a growth isotherm and first appearance of crystals (nucleation lag time) is related to the proximity of the growth isotherm to the liquidus of the bulk composition. For example, no nucleation appeared in the run products after 144 hours at 850°C or 24 hours at 800°C for the bulk composition labeled *b* on Figure 2, whereas an experiment of 48 hours at 800°C produced crystals.

Nucleation of a solid from a melt without the aid of foreign materials, such as nuclei or container walls, is termed homogeneous nucleation and is contrasted to heterogeneous nucleation where the crystals nucleate on some foreign substrate (Flemmings, 1974). Homogeneous nucleation is difficult to prove, since the nuclei are submicroscopic. Capsule walls sometimes provide a substrate for spherulite nucleation. When crystals nucleate on capsule walls, they produce larger crystals than the crystals that nucleated within the charge, indicating that the larger crystals (externally nucleated crystals) may nucleate before the smaller crystals within the charge (internally nucleated crystals). Such externally nucleated crystals are not used in the nucleation or growth-rate curves of Figures 2–3.

Vapor bubbles might be expected to act as sites for heterogeneous nucleation. Bubbles of an H_2O-rich vapor phase are present in charges of certain bulk compositions. Presence of these bubbles did not affect the nucleation of either the feldspars or quartz.

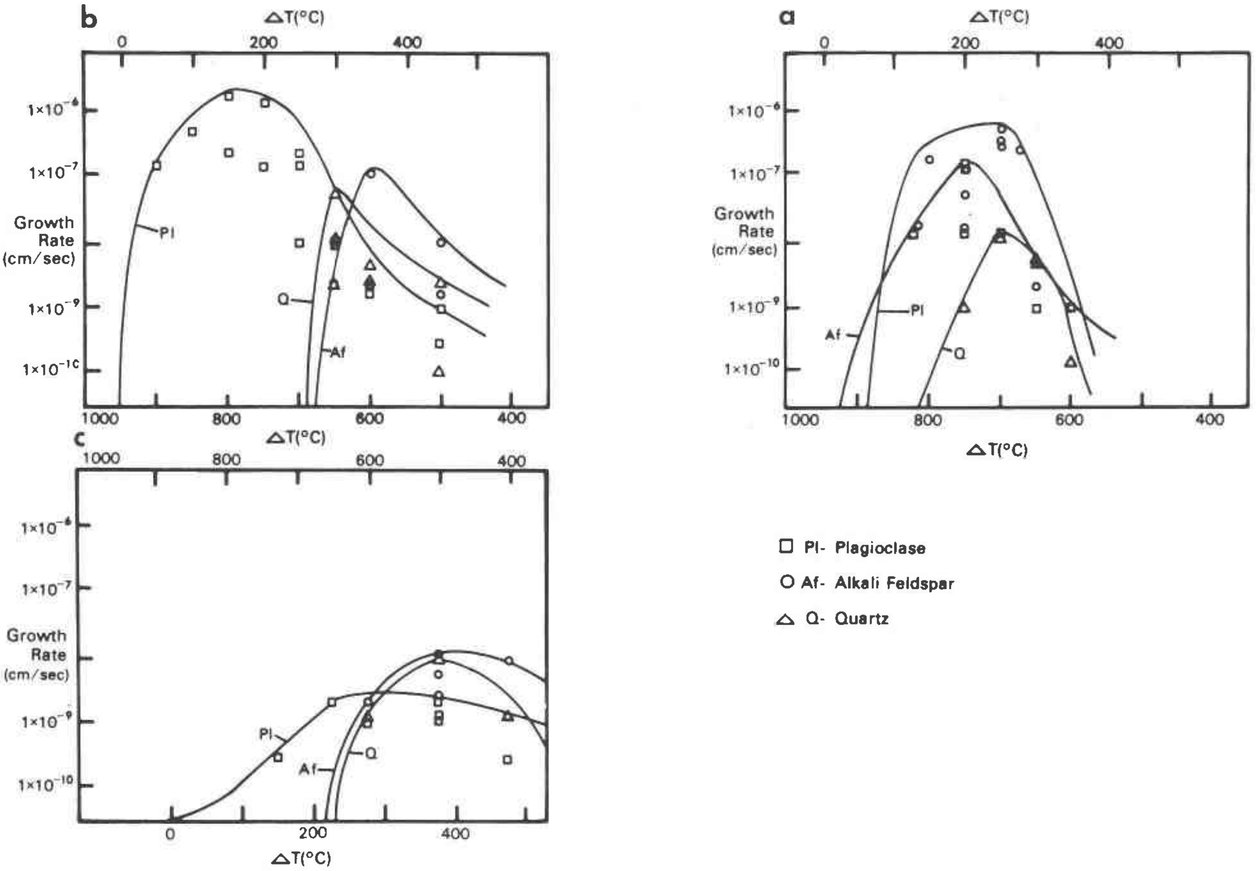

Fig. 3. Crystal-growth rates as a function of undercooling (Δ*T*). (a) Synthetic granite plus 3.5 wt % H_2O. (b) Synthetic granodiorite plus 6.5 wt % H_2O. (c) Synthetic granodiorite plus 12 wt % H_2O.

Some very small crystals are observed on the inside walls of the vapor bubbles, but these are presumed to be material that was dissolved in the vapor and crystallized on the quench to room temperature. Bubbles did not act as nucleation sites for feldspars or quartz and are not found in the center of any of these crystals.

Generalizations regarding the nucleation density curves are difficult. Tammann (1925) showed that nucleation would rise to a maximum and then fall with increased undercooling. This same nucleation pattern is found for the granitic systems (Fig. 2). The maximum density of nucleation sites is approximately the same in the granodiorite system, whereas the granite with 3.5 weight percent water has a maximum nucleation density an order of magnitude greater (Fig. 2).

Within a melt the number of nuclei is dependent upon temperature, and this fact may be used to explain the time between quench to a growth isotherm and nucleation of crystals. Quench to a growth temperature causes a rapid decrease in temperature within the system, and the distribution of nuclei must readjust to this new temperature before nucleation can start (Turnbull, 1948). This period of readjustment may explain the nucleation lag time.

Table 2. Example of experimental results from the synthetic granodiorite with 6.5 wt % H_2O crystallized at 800°C (Δ*T* = 150°)

Growth Time (hrs)	Charge #	Nucleation Density (Sites/cm^3)	Growth Rate (cm/sec)
24	1052	NN*	———
24	1053	31**	2.7x10-6
48	1790	NN	———
48	1791	NN	———
96	1268	31	7.8x10-7
144	1461	31	2.1x10-7
144	1463	62	4.0x10-7

* NN - No nucleation
** Corresponds to 1 nucleation site per charge

Crystal-growth rate

When the charges were examined after the experiment, the maximum amount of crystal growth was determined, and this was divided by the amount of time allowed for crystal growth to obtain the growth rate. Measurement of the amount of crystal growth for spherulites was relatively simple, since the center of the spherulite where crystallization started could be easily identified. For charges containing individual crystals one half of the crystal length is assumed to be the amount of growth. The largest problem in this method is a lack of data on the exact length of time involved in the crystal growth. For example, if a charge does not nucleate any crystals in a 24 hour experiment but does nucleate crystals in a 48 hour experiment, what is the time of growth? All of the growth in the 48 hour run could have occurred in the last 6 hours or even 6 minutes. Because growth times are not exactly known, the growth rates on Figure 3 represent minimum values. At the highest growth rates, crystals often hit the side of the capsule or other crystals, and this interferes with the length of growth and acts to reduce the calculated growth rate.

Growth-rate curves shown on Figure 3 are drawn to include all the data points from internally nucleated crystals. Scatter in the growth-rate data can be clearly seen on Figure 3. Growth rates measured on externally nucleated crystals were greater than the growth rates for internally-nucleated crystals; this supports the idea of faster nucleation (and hence longer growing time) for the crystals nucleated on foreign materials.

Growth-rate data suffer largely from a lack of knowledge concerning the amount of time involved in the growth of a given crystal, but other factors may contribute errors. Interpretation of the textural relations can introduce another source of error in determination of growth rate. For example, in a semiradial arrangement of crystals, did a given crystal start growth at one end or did it start growth in the center and grow in both directions? The assumed answer will make a factor-of-2 difference in the growth rate.

Several generalizations can be made with regard to the growth rates measured in this study. As the amount of undercooling increases, the growth rate for an individual phase increases to a maximum and then decreases (Fig. 3). This is the expected behavior of growth rate measured in a viscous liquid (Tammann, 1925). With a given anhydrous bulk composition, the maximum growth rate decreases as the amount of water in the system increases (Fig. 3). Fenn (1976) also observed a decrease in the maximum growth rate with increasing water content, and this relation is as yet unexplained. Addition of water to a silicate system lowers the viscosity of the silicate liquid (Friedman *et al.,* 1963; Shaw, 1963). A greater mobility of components and hence a faster crystal growth rate is expected as a result of lowered viscosity. Decrease in crystal-growth rate with increasing water content is not compatible with the petrogenetic theory equating the growth of large crystals with the evolution of a vapor phase (Jahns and Burnham, 1958).

A note of caution must be issued about the plots shown of Figures 2 and 3. Within spherulites, individual phases are very difficult and sometimes impossible to identify. Spherulitic growth is dominant at small undercoolings in the granite composition and is also found within the granodiorite composition.

Given this limitation on phase identification in spherulites, the results shown of Figures 2 and 3 are probably more accurate for the granodiorite than the granite systems, and more reliable at larger undercoolings within the granite system. However, it is felt that the results presented on Figures 2 and 3 represent a vast improvement over nucleation and growth-rate plots that are schematic (Dowty *et al.,* 1974; Carmichael *et al.,* 1974) despite any limitations on the absolute numbers.

Textural relations

Texture describes the relations of crystals and glass in these experiments in terms of size, shape, and arrangement. Crystal morphology refers to the shape of individual crystals and, as explained previously, is controlled by the growth rate and the diffusivity of the least mobile component in the system. Crystal morphology should thus vary with undercooling (Kirkpatrick, 1975). Since nucleation and growth rate also vary with undercooling, textures are expected to vary with undercooling.

A radial array of crystals is the most commonly observed texture in the hypersolidus region of the bulk compositions studied. The radial array may involve the large crystals found in the granodiorite composition at low undercoolings (Fig. 4) or classical spherulite development seen in the synthetic granite and any combination in between. Indeed no clear boundary exists between any of the crystal morphologies observed in this study. With an increase in undercooling, large single crystals give way to an open array of coarse skeletal to dendritic crystals, and finally a more compact radial mass of coarse

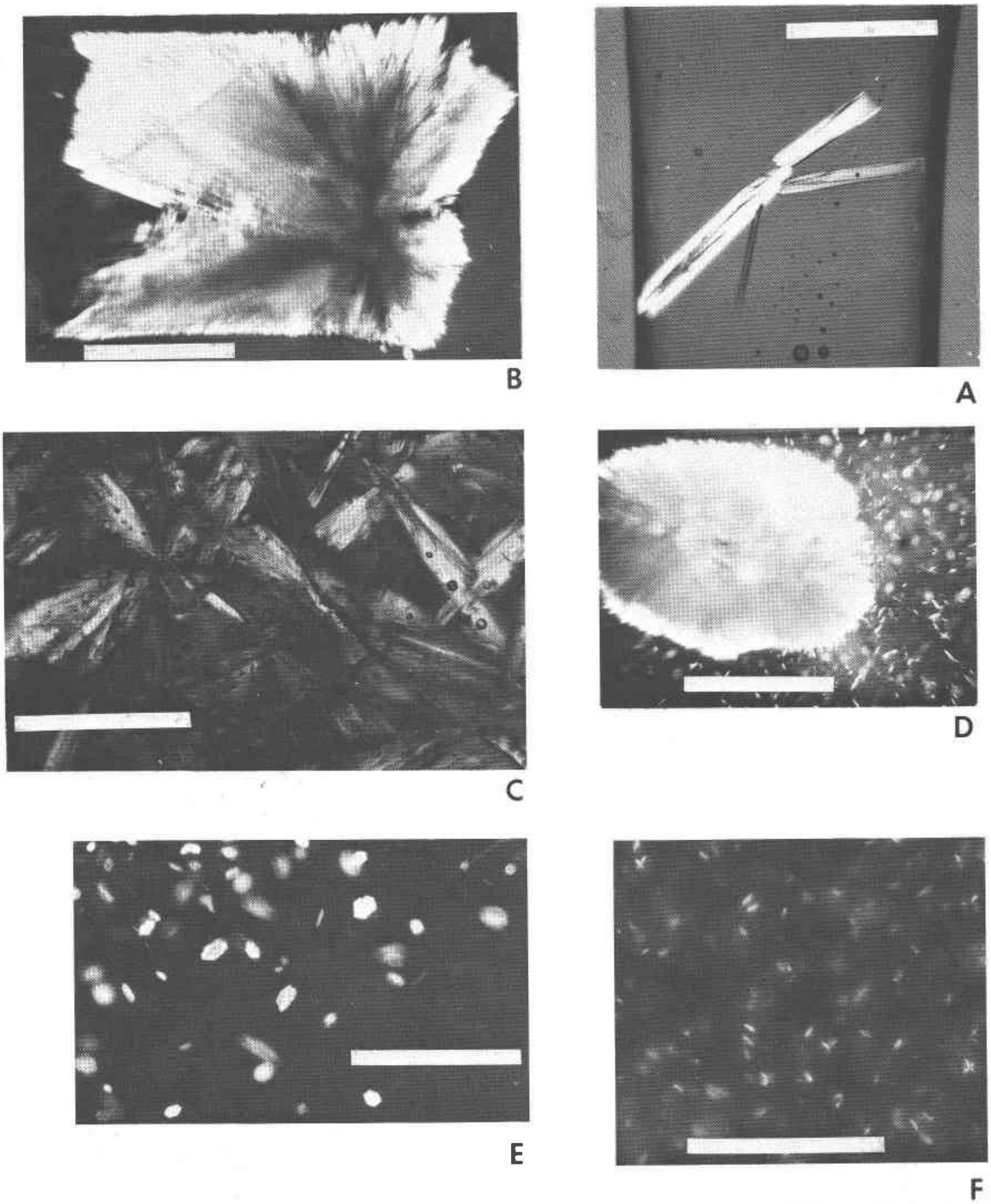

Fig. 4. Photomicrographs of synthetic granodiorite plus 6.5 wt % H_2O. (a) Plagioclase crystals, $\Delta T = 50°C$, crystallization time 144 hrs. White bar is 1.0 mm. (b) Plagioclase spherulite, $\Delta T = 150°C$, crystallization time 24 hrs. White bar is 1.0 mm. (c) Dendritic plagioclase crystals, $\Delta T = 150°C$, crystallization time 144 hrs. White bar is 0.25 mm. (d) Spherulite of plagioclase with smaller crystals of alkali-feldspar, $\Delta T = 300°C$, crystallization time 24 hrs. White bar is 1.0 mm. (e) Crystals of quartz (hexagonal plates) and alkali-feldspar (tabular crystals), $\Delta T = 300°C$, crystallization time 24 hrs. White bar is 0.25 mm. (f) Crystals of quartz, alkali-feldspar, and plagioclase, $\Delta T = 350°C$, crystallization time 24 hrs. White bar is 0.1 mm.

crystals results (Fig. 4). This same sequence of crystal morphologies has been observed in other experimental studies (Lofgren 1974a, Fenn 1976) and in rocks (Bryan, 1972) and is directly related to the amount of undercooling (Kirkpatrick, 1975).

Plagioclase and alkali-feldspar crystals grown in this study show the same growth forms as the alkali-feldspars grown by Fenn (1973, 1976). This is not surprising in view of the slight structural difference between the alkali and the plagioclase feldspars. Crystals are elongated parallel to the *a* axis with the elongate sides bounded by (001) and terminated by the (100) face. Relative growth velocities along the axes are $a > c > b$.

Quartz crystals grown in this study commonly lie on the (0001) plane, resulting in hexagonal plates, although some crystals are elongated parallel to the *c* axis. Relative growth rates for the different orientations of quartz are $c > a$.

Radial masses show growth along a preferred crystallographic axis, low angle branching of crystals, and a distinctive extinction cross. All these properties are characteristic of spherulitic growth (Keith and Padden, 1963). Development of spherulites is to be expected from these melts due to the high viscosity, slow growth rate, and low number of nuclei (Keith and Padden, 1963). Even for the small crystals, formed at large undercoolings (400–500°C), high magnification reveals the fibrous nature of the crystals. These small fibrous crystals probably represent small spherulites. Within a crystal, individual fibers have the same crystallographic orientation. Crystals composed of individual fibers are not a common feature of igneous rocks, and presumably with further heating the fibers will anneal to form single solid crystals.

The patterns of crystallization for the synthetic granite and granodiorite are quite different. In the granodiorite composition, crystallization of large crystals is followed by dendritic morphologies, spherulite crystallization, and finally growth of small fibrous single crystals with increased undercooling (Figure 4). In the synthetic granite the crystallization of spherulites is followed by small fibrous crystals with increasing undercooling, the large crystals found in the granodiorite at small undercoolings are not found in the granite.

Temperature is a logical variable to explain the change in crystal morphologies. Crystal morphologies show a progressive change with undercooling; on the basis of crystal growth in the system $NaAlSi_3O_8$–$CaAl_2Si_2O_8$–H_2O Lofgren (1974a) proposed a general relationship between crystal morphology and undercooling, *viz.*, that plagioclase crystallized from a silicate melt will show a change from tabular to skeletal and dendritic growth forms and finally result in a spherulitic morphology with increased undercooling. Care was taken to describe the crystal morphologies, and the gradual change from one morphology to another was also noted, although for sodium-rich bulk compositions the plagioclase crystals showed a change from tabular directly to spherulitic morphologies apparently without any intermediate growth forms. The pattern of crystallization observed in the granodiorite in this study is similar to the pattern suggested by Lofgren. He did not observe very small crystals, but this could be attributed to a lack of sufficient undercooling. The crystallization sequence of spherulites to small fibrous crystals observed in the synthetic granite omits the tabular, skeletal, and dendritic morphologies that Lofgren includes in his description of crystal-growth forms.

Development of igneous textures

Textures resulting from the crystallization of a silicate melt are dependent upon the crystal nucleation and growth rate, and these parameters vary with the temperature–pressure path followed by the melt during crystallization. Addition of iron and magnesium will add new phases to these systems and thus change the kinetics of nucleation and growth (Naney, 1975), but the generalities developed here for feldspars and quartz should hold true for these systems even with a small quantity of mafic components.

Observation of growth of reasonably large crystals (several millimeters) in a short period of time geologically (several days) is one of the most significant results of this study. Such growth rates are found in systems containing one crystalline phase (Mustart, 1972; Fenn, 1973, 1976; Lofgren, 1974b), but this is the first time such growth rates have been measured in the polyphase granitic systems. Rapid crystallization of feldspar and quartz in these systems suggests reevaluation of the length of time required to produce the large crystals of the granitic rocks. Increase in water content produces a decrease in the maximum apparent growth rate for the system (Fig. 3), and this should lead to a reinterpretation of the role of the vapor phase in producing large crystals.

Textures of igneous rocks are controlled largely by the kinetics of nucleation and growth of the crystals. For the compositions used in this study, crystallization at small undercoolings produces relatively few nucleation sites with large crystals, as is characteristic of plutonic rocks, whereas large undercoolings produce a large number of nucleation sites with small crystals, as found in volcanic rocks. Obviously such extremes of temperature change are rarely found, and more commonly, plutonic rocks crystallize from a slightly undercooled melt that is continuing to cool. This would result in a texture in which different phases would have different grain sizes, depending on the nucleation and growth rates. Zoning would also be expected in phases of variable composition. Volcanic rocks often contain phenocrysts set in a fine-grained groundmass, and this texture has been interpreted as resulting from movement of a magma that was crystallizing at a low undercooling with a few nucleation sites to an environment with a lower undercooling to produce the fine-grained groundmass. Similar models have been developed to explain the porphyritic textures in intrusive igneous rocks.

Combination of the experimental results shown on Figures 2 and 3 (Fig. 5) suggests an interesting model for the development of porphyritic textures in granodioritic compositions. At low undercooling temperatures, plagioclase has a rapid growth rate and a low nucleation density, which may lead to formation of a few large, euhedral plagioclase crystals. Continued crystallization at greater undercoolings would result in these plagioclase crystals being a substrate for new growth, in addition to the growth produced on new plagioclase nucleation sites. Plagioclase crystals nucleated early in the crystallization process would have large euhedral cores, whereas crystals that nucleated later would have smaller, more irregular cores, due to interference with other crystals and a slower growth rate (Fig. 4).

Plagioclase does not commonly form phenocrysts in granodiorites, and yet the high growth rate combined with a relatively small number of nuclei at low undercoolings suggests ideal conditions for their development. There may be several reasons for the lack of plagioclase phenocrysts in granodiorites. Crystals formed early in the cooling process may be removed from the liquid by some differentiation process. Decrease in growth rate coupled with an increase in the number of nuclei may mask the early plagioclase crystals during later crystallization. Finally, most granodiorite magmas may never be entirely liquid, but instead consist of a mixture of crystals (including plagioclase) and liquid. In this case, crystallization would not produce the few large plagioclase crystals predicted from Figure 5; instead the early crystallization would take place on a substrate of preexisting plagioclase crystals. However, in some dikes (Bateman and Wahrhaftig, 1966) plagioclase phenocrysts are found in granodiorites, and these occurrences are easily explained using the information on Figure 5.

Development of alkali-feldspar phenocrysts in granodiorites and adamellites has been discussed by Bateman *et al.* (1963) and Kerrick (1969). Phenocrysts vary widely in size, the largest being over 10 cm in length. Morphology of the phenocrysts ranges from euhedral to anhedral in different plutons. Inclusions of other minerals are found within the phenocrysts in zones paralleling the crystal faces of the alkali-feldspar crystals. The mineral inclusions appear to have been pushed out in front of and finally included in the advancing face of the alkali-feldspar phenocryst, suggesting that these phenocrysts developed while there was at least some silicate liquid remaining in the system. Movement of water in front of an advancing alkali-feldspar crystal face has been described by Fenn and Luth (1973), and the development of concentration gradients in front of an advancing crystal face seems a reasonable explanation for the inclusions in the alkali-feldspar phenocrysts, and supports a model of crystallization from a silicate liquid.

Development of alkali-feldspar phenocrysts in granodiorites may be explained from the relation of the nucleation density and growth rate curves for alkali-feldspar shown on Figure 5. The growth rate of the alkali-feldspar reaches a maximum while the nucleation density for this phase is relatively low. Development of a few large alkali-feldspar phenocrysts is expected from the granodioritic magma. Maximum development of the alkali-feldspar phenocrysts is expected near the solidus temperature under these pressure conditions (Figs. 1 and 5). Alkali-feldspar phenocrysts may push other phases aside during growth or include these preexisting phases within the phenocrysts. In some cases the magma may be nearly solid when the alkali-feldspar starts to crystallize, and due to the limited space, these phenocrysts would be anhedral and even interstitial. Based on the crystallization kinetics of alkali feldspar in granodioritic magmas, phenocrysts of this late-crystallizing phase are expected in granodiorites.

Development of large crystals of quartz in granodiorites is not expected. Maximum growth of quartz corresponds with the maximum in nucleation density, and this combination would produce a large number of relatively small quartz grains. A similar argument may be made for all of the crystalline phases in the synthetic granite.

Crystallization kinetics of the granite systems have been combined from Figures 2 and 3 and are shown in Figure 5. Maximum growth rates and nucleation densities coincide for quartz and plagioclase in the granite composition (Fig. 5). As in the case of quartz in the granodiorite system, coincidence of high nucleation densities and growth rates results in crystallization of many relatively small crystals. The high growth rate of alkali-feldspar might be expected to produce large crystals in the granite system (Fig. 5). Nucleation density is high for all phases, and the growth rate of the alkali-feldspar is two orders of magnitude greater than growth rates measured on other crystalline phases. Under these conditions the alkali-feldspar is expected to be much larger than the other crystals. From these results, granites crystallized at low undercoolings are expected to form alkali-feldspar phenocrysts while granites crystallized at large undercooling temperatures will be equigranular. Bateman *et al.* (1963) have found that the granites of the Sierra Nevada batholith in California are equigranular, although Williams *et al.* (1954) find alkali-feldspar phenocrysts common in granites. Based on the crystallization kinetics shown in Figure 5, either equigranular or porphyritic rocks are expected from granite systems, depending on the undercoolings.

Conclusions

Textures of igneous rocks are largely dependent upon the crystallization kinetics of the system. Development of nuclei and the subsequent rate of growth will determine the appearance of individual crystalline phases. Since the texture of a rock is the mosaic of mineral grains, igneous-rock textures will be determined by the crystal-growth kinetics of the individual phases. Crystallization kinetics of a particular phase vary from one bulk composition to another, and this helps to explain why different igneous rocks sometimes show different textures.

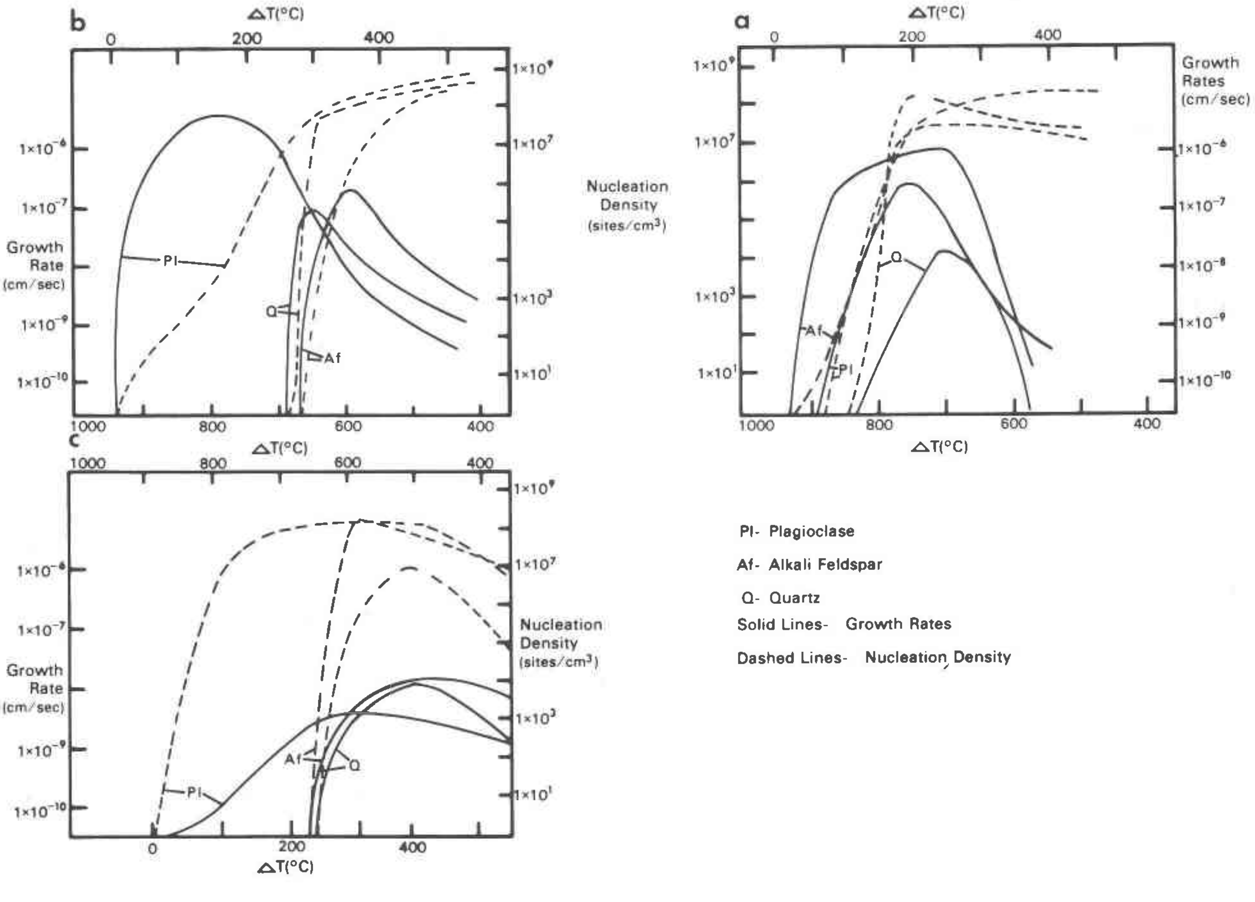

Fig. 5. Combined nucleation density and crystal-growth rate curves. (a) Synthetic granite plus 3.5 wt % H_2O. (b) Synthetic granodiorite plus 6.5 wt % H_2O. (c) Synthetic granodiorite plus 12 wt % H_2O.

This study is concerned with the concept of time of crystallization and texture in igneous rocks. Conceptually, plutonic rocks are coarse-grained because of long periods of slow cooling and crystallization, whereas volcanic rocks are fine grained because of very rapid cooling and crystallization. Nucleation density and growth-rate plots shown on Figure 5 offer an alternative explanation for the development of plutonic and volcanic textures. Crystal-growth rates within these systems reach maximum values on the order of several millimeters per day. Obviously, at this rate long time periods are not needed to produce the type of crystals characteristic of plutonic rocks. This does not imply that temperatures within the earth fall so much [T(liquidus) $-$ T(solidus) $\approx 300°$] in such a short period of time, but it does illustrate that long time periods are not *necessary* for the development of plutonic textures. Rapid crystallization to produce a plutonic texture may account for the plutonic rocks that crystallized at shallow depths in some volcanic areas (Tabor and Crowder, 1969).

Volcanic textures result when magma is quickly subjected to large undercooling temperatures by extrusion. Figure 5 shows that at large undercooling values, nucleation density is high and growth rate is low, which produces a large number of small crystals. Volcanic textures are produced by the crystallization kinetics at large undercooling values.

Development of porphyritic textures depends on the association of a low nucleation density and a rapid growth rate. Phenocrysts have been described as minerals that crystallized early and were carried with the magma to a new environment, resulting in rapid crystallization of the groundmass. However, the possible development of phenocrysts of alkalifeldspar in granodiorites has been previously discussed, and that model does not depend on any two-stage crystallization process. "Porphyritic" textures were produced in a number of charges in this study in a one-step crystallization, where larger grains of a faster-growing phase coexist with smaller grains of a slower growing phase (Figure 4). Development of temperature-induced zoning is found in many phenocrysts. In the absence of this type of corroborating evidence, there is little reason to believe that a porphyritic texture was produced during a multistage crystallization process.

Crystallization kinetics involving the nucleation and growth of crystals in magmas are important tools in understanding the development of igneous textures. Extension of this type of study to other systems will furnish valuable information on the development of textures in other types of igneous rock.

Acknowledgments

The author thanks W. C. Luth and P. M. Fenn for assistance and advice during the course of this study. Special thanks are due to P. R. Gordon for technical assistance in the operation and maintenance of the high pressure equipment. P. M. Fenn, H. R. Shaw, and an anonymous reviewer made many helpful comments on an early version of this manuscript. This work was supported by NSF grants GA 1684 (to R. H. Jahns and W. C. Luth) and GA 41731 (to W. C. Luth, G. E. Brown and W. A. Tiller).

References

Akella, J. and C. G. Kennedy (1971) Melting of gold, silver, and copper—proposal for a new high-pressure calibration scale. *J. Geophys. Res.*, *76*, 4969–4977.

Bateman, P. C., L. D. Clark, N. K. Huber, J. G. Moore and C. D. Rinehart (1963) The Sierra Nevada batholith—a synthesis of recent work across the central part. *U.S. Geol. Surv. Prof. Pap. 414-D.*

———, and C. Wahrhaftig (1966) Geology of the Sierra Nevada. In E. H. Bailey, Ed., *Geology of Northern California*, p. 107–172. *Calif. Div. Mines Geol. Bull. 190.*

Bryan, W. B. (1972) Morphology of crystals in submarine basalts. *J. Geophys. Res.*, *77*, 5812–5819.

Cahn, J. W. (1967) On the morphological stability of growing crystals. In H. S. Peiser, Ed., *Crystal Growth*, p. 681–690. Pergamon Press, Oxford.

Carmichael, I. S. E., F. J. Turner and J. Verhoogen (1974) *Igneous Petrology*. McGraw-Hill, New York.

Clark, S. P., Jr. (1959) Effect of pressure on the melting points of eight alkali halides. *J. Chem. Phys.*, *31*, 1526–1531.

Donaldson, C. H. (1974) Experimental investigation of olivine morphology (abstr.). *Geol. Soc. Am. Abstr. Progr.*, *6*, 712.

Dowty, E., K. Keil and P. Martin (1974) Lunar pyroxene-phyric basalts: crystallization under supercooled conditions. *J. Petrol.*, *15*, 419–454.

Fenn, P. M. (1972) Nucleation and growth of alkali feldspars from synthetic melts (abstr.). *Trans. Am. Geophys. Union*, *53*, 1127.

——— (1973) *Nucleation and Growth of Alkali Feldspars from Melts in the System* $NaAlSi_3O_8$–$KAlSi_3O_8$–H_2O. Ph.D. Thesis, Stanford University, Stanford, California.

——— (1976) Nucleation and growth of alkali feldspar from hydrous melts. *Can. Mineral.*, in press.

———, and W. C. Luth (1973) Hazards in the interpretation of primary fluid inclusions in magmatic minerals (abstr.). *Geol. Soc. Am. Abstr. Progr.*, *5*, 617.

Flemmings, M. C. (1974) *Solidification Processing*. McGraw-Hill, New York.

Friedman, I., W. Long and R. L. Smith (1963) Viscosity and water content of rhyolite glass. *J. Geophys. Res.*, *68*, 6523–6535.

Gibb, F. G. F. (1974) Supercooling and the crystallization of plagioclase from a basaltic magma. *Mineral. Mag.*, *39*, 641–653.

Jahns, R. H. and C. W. Burnham (1958) Experimental studies of pegmatite genesis: melting and crystallization of granite and pegmatite (abstr.) *Geol. Soc. Am. Bull.*, *69*, 1592–1593.

Keith, H. D. and F. J. Padden Jr. (1963) A phenomenological theory of spherulite crystallization. *J. Appl. Phys.*, *34*, 2409–2421.

Kerrick, D. M. (1969) K-feldspar magacrysts from a porphyritic quartz monzonite, central Sierra Nevada, California. *Am. Mineral.*, *54*, 839–848.

Kirkpatrick, R. J. (1974) Kinetics of crystal growth in the system $CaMgSi_2O_6$–$CaAl_2SiO_6$. *Am. J. Sci.*, *274*, 215–242.

——— (1975) Crystal growth from the melt: a review. *Am. Min-*

eral., *60*, 798–814.

———, C. R. Robinson and J. F. Hays (1975) Kinetics of crystal growth from silicate melts: diopside and anorthite (abstr.). *Geol. Soc. Am. Abstr. Progr.*, *7*, 1147.

Lofgren, G. E. (1974a) An experimental study of plagioclase crystal morphology: isothermal crystallization. *Am. J. Sci.*, *274*, 243–273.

——— (1974b) Temperature induced zoning in synthetic plagioclase feldspar. In W. S. MacKenzie and J. Zussman, Eds., *The Feldspars*, p. 362–376. Manchester Univ. Press, Manchester.

———, R. J. Williams, C. H. Donaldson and T. M. Usselman (1975) Experimental investigation of porphyritic texture (abstr.). *Geol. Soc. Am. Abstr. Progr.*, *7*, 1173–1174.

Luth, W. C. and C. O. Ingamells (1965) Gel preparation for hydrothermal experimentation. *Am. Mineral.*, *50*, 255–258.

Meiling, G. S. and D. R. Uhlmann (1967) Crystallization and melting kinetics of sodium disilicate. *Phys. Chem. Glasses*, *8*, 62–68.

Mustart, D. A. (1969) Hydrothermal synthesis of large single crystals of albite and potassium feldspar (abstr.). *Trans. Am. Geophys. Union*, *50*, 675

——— (1972) *Phase Relations in the Peralkaline Portion of the System* Na_2O–Al_2O_3–SiO_2–H_2O. Ph.D. Thesis, Stanford University, Stanford, California.

Naney, M. T. (1975) Nucleation and growth of biotite and clinopyroxene from haplogranitic magmas (abstr.). *Trans. Am. Geophys. Union*, *56*, 1075.

Nockolds, S. R. (1954) Average chemical composition of some igneous rocks. *Geol. Soc. Am. Bull.*, *65*, 1007–1032.

Shaw, H. R. (1963) Obsidian-H_2O viscosities at 1000 and 2000 bars in the temperature range 700° to 900°C. *J. Geophys. Res.*, *68*, 6337–6343.

Swanson, S. E. (1974) The effect of crystal growth rate and nucleation density on the texture of granodiorites (abstr.). *Geol. Soc. Am. Abstr. Progr.*, *6*, 979.

———, J. A. Whitney and W. C. Luth (1972) Growth of large quartz and feldspar crystals from synthetic granitic liquids (abstr.). *Trans. Am. Geophys. Union*, *53*, 1127.

Tabor, R. W. and D. F. Crowder (1969) On batholiths and volcanoes—intrusion and eruption of late Cenozoic magmas in the Glacier Peak area, north Cascades, Washington. *U.S. Geol. Surv. Prof. Pap.*, *604*.

Tammann, G. (1925) *The States of Aggregation.* Van Nostrand, New York.

Towers, H. and J. Chipman (1957) Diffusion of calcium and silicon in a lime–alumina–silica slag. *Trans. Am. Inst. Min. Eng.*, *209*, 769–773.

Turnbull, D. (1948) Transient nucleation. *Trans. Am. Inst. Min. Eng.*, *175*, 774–783.

Vogt, J. H. L. (1923) The physical chemistry of the crystallization and magmatic differentiation of igneous rocks: VII viscosity, influence of time, undercooling (or supersaturation), and equilibrium of mix-crystals between the solid and liquid phase, *etc. J. Geol.*, *31*, 233–252.

Whitney, J. A. (1975) The effects of pressure, temperature, and X_{H_2O} on phase assemblage in four synthetic rock compositions. *J. Geol.*, *83*, 1–31.

Williams, H., F. J. Turner and C. M. Gilbert (1955) *Petrography; An Introduction to the Study of Rocks in Thin Sections.* Freeman, San Francisco.

Winkler, H. G. F. (1947) Kristallogrosse und Abkuhlung. *Heidelberger Beitr. Mineral. Petrol.*, *1*, 86–104.

Wyllie, P. J. (1963) Applications of high pressure studies to the earth sciences. In, R. S. Bradley, Ed., *High Pressure Physics and Chemistry*, Vol. 2. Academic Press, New York.

Yoder, H. S., Jr. (1950) High-low quartz inversion up to 10,000 bars. *Trans. Am. Geophys. Union*, *31*, 827–835.

Manuscript received, February 4, 1976; accepted for publication, March 31, 1977.